Int J Thermophys (2009) 30:9–19
DOI 10.1007/s10765-008-0459-0

# Design and Evaluation of Large-Aperture Gallium Fixed-Point Blackbody

**V. B. Khromchenko · S. N. Mekhontsev · L. M. Hanssen**

Published online: 6 June 2008


**Abstract** To complement existing water bath blackbodies that now serve as NIST primary standard sources in the temperature range from 15 °C to 75 °C, a gallium fixed-point blackbody has been recently built. The main objectives of the project included creating an extended-area radiation source with a target emissivity of 0.9999 capable of operating either inside a cryo-vacuum chamber or in a standard laboratory environment. A minimum aperture diameter of 45 mm is necessary for the calibration of radiometers with a collimated input geometry or large spot size. This article describes the design and performance evaluation of the gallium fixed-point blackbody, including the calculation and measurements of directional effective emissivity, estimates of uncertainty due to the temperature drop across the interface between the pure metal and radiating surfaces, as well as the radiometrically obtained spatial uniformity of the radiance temperature and the melting plateau stability. Another important test is the measurement of the cavity reflectance, which was achieved by using total integrated scatter measurements at a laser wavelength of 10.6 μm. The result allows one to predict the performance under the low-background conditions of a cryo-chamber. Finally,

Certain commercial equipment, instruments, or material are identified in this paper to specify the experimental procedures and result adequately. Such identification is not intended to imply recommendation or endorsement by the National Institute of Standards and Technology, nor is it intended to imply that material or equipment identified are necessarily the best available for the purpose.

V. B. Khromchenko
Space Dynamics Laboratory, North Logan, UT 84341, USA

V. B. Khromchenko (✉)
Joint NIST/USU Program in Optical Sensor Calibration, North Logan, UT, USA
e-mail: vladimir.khromchenko@nist.gov

S. N. Mekhontsev · L. M. Hanssen
Optical Technology Division (844), National Institute of Standards and Technology, 100 Bureau Drive, Stop 8442, Gaithersburg, MD 20899-8442, USA

results of the spectral radiance comparison with the NIST water-bath blackbody are provided. The experimental results are in good agreement with predicted values and demonstrate the potential of our approach. It is anticipated that, after completion of the characterization, a similar source operating at the water triple point will be constructed.

**Keywords** Blackbody · Emissivity · Fixed point · Gallium

## 1 Introduction

The development of new blackbody (BB) sources operating in the near-ambient background temperature range for calibration of remote sensing or thermal-imaging systems with a total uncertainty of 0.1% is one of the main objectives for radiometric standards development [1]. Many applications require a compact, extended-area standard BB for near-ambient temperature operating both in cryo-vacuum and in the open air. An extended-area water-bath BB is well suited for many applications because of its excellent temperature uniformity and stability, but it can be used only in air [2]. In addition, there is a need for blackbodies that are linked to primary standards operating under ambient conditions.

The phase transition of gallium enables the construction of a BB that does not depend on, or requires, high-quality platinum resistance thermometers. In the past, it has been demonstrated that it is possible to build a high-quality gallium blackbody with a small aperture that can operate in vacuum [3] or in the open air [4]. To reduce the influence of background conditions on a BB output, one can decrease the radiation losses through the BB cavity aperture by installation of a concentrator of radiation in front of the cavity. In this article, we describe the construction and realization of a large-area BB with a reflecting concentrator based on the gallium phase-transition temperature, which has a defined melting-point temperature of 29.7646 °C on the International Temperature Scale of 1990 (ITS-90).

## 2 Design and Construction

The design of our gallium fixed-point BB that is capable of operation in both vacuum and open air is shown in Fig. 1. The BB cavity is constructed using a copper conical shell which is coated with Chemglaze Z302* [5] specular black paint. The gallium cannot directly contact the copper cavity because of contamination issues; hence, it is contained in a Teflon cell. The thickness of the Teflon wall around the cone is kept to a minimum value of 1.4 mm. A thermistor, located in the cavity wall close to the opening, enables monitoring of the cavity temperature during melt/freeze sequences, as well as use of the BB in a variable-temperature mode of operation. The gallium cell is enclosed in a solid copper heat exchanger with brazed pipes attached for heat exchange with a fluid, supplied via a vacuum feedthrough at the rear flange of the BB case. Under normal laboratory conditions, BB operation can be controlled by any refrigerated circulating bath. An additional electrical heater, wound around

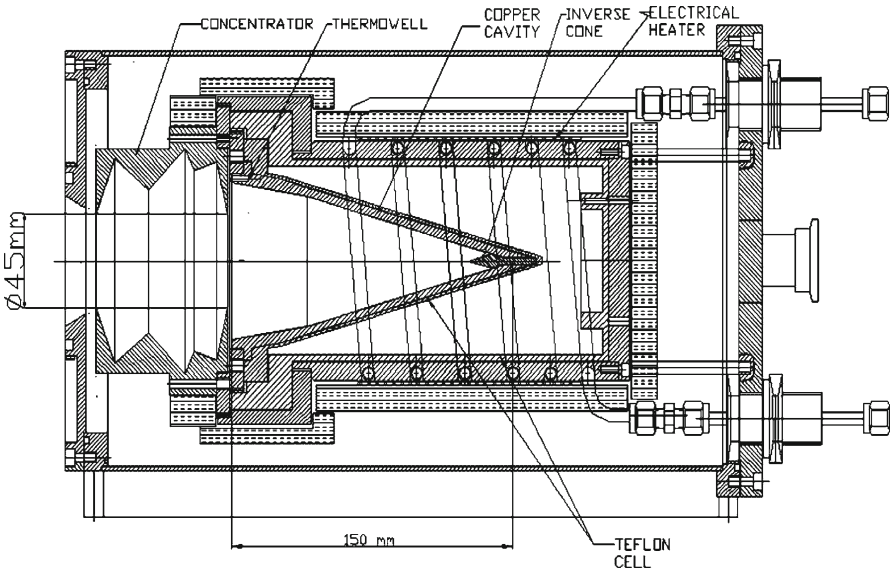


**Fig. 1** Schematic of the gallium melting-point BB

the heat exchanger, enables operation of the BB inside a low-temperature vacuum chamber without use of a heat transfer fluid. A second thermistor is attached to the outer surface of the heat exchanger to monitor its temperature. The Teflon cell inside the heat exchanger contains approximately 5 kg of 0.999999 purity gallium. The heat exchanger is wrapped in multiple layers of foil insulation and fixed on the rear flange with four stainless-steel rods inside a vacuum-tight case. For operation in vacuum, the front flange of the case can be flanged to a vacuum chamber, or the entire BB can be mounted on a heat sink inside the vacuum chamber.

To avoid the formation of a meniscus during painting of the copper cone, we drilled a small hole at its apex and closed it with an inner inverse cone that fits tightly against the main cone. To improve the thermal coupling between the Teflon cell and the copper cavity, vacuum grease was used.

## 3 Cavity Geometry for Optimal Emissivity

The shape of the copper cavity was selected to be similar to the one used in our water-bath BB [2]. The apex angle of the conical bottom was optimized to obtain a maximum of the normal effective emissivity, taking into account the spectral reflectance of the Z302 paint. As shown in Fig. 2, for constant linear dimensions of the cavity, the conical bottom apex angle $\beta$ was a parameter. Calculations of the emissivity were performed by the Monte Carlo method according to the algorithm described in [6]. The results of the calculations are presented in Fig. 3; the actual apex angle $\beta$ was chosen to be 32°. Addition of the inverse inner cone does not affect the calculated emissivity.

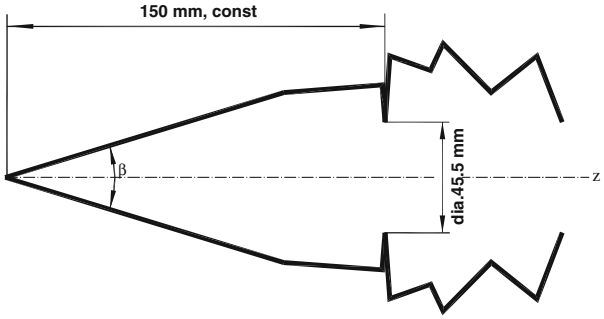


**Fig. 2** Copper cavity geometry, $\beta$ is the apex angle

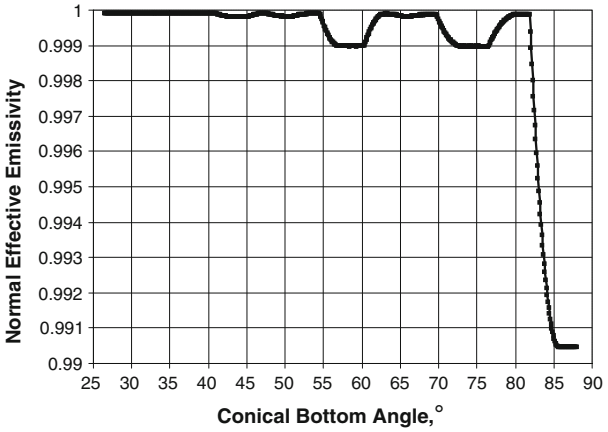


**Fig. 3** Calculated emissivity of the cone without the reflector vs. apex angle

A key element in the design of blackbodies with an extended aperture is a way to reduce the radiation losses through the cavity aperture. This is primarily achieved by either lengthening the cavity or using a reflecting concentrator (Fig. 4).

It is known [7,8] that the effective emissivity of radiators can be increased with the aid of a hemispherical reflecting concentrator with an opening for the radiation to exit. Since a hemispherical mirror substantially increases the dimensions of a radiating system, it is reasonable to replace it with another reflecting concentrator, even at the expense of a small decrease in the effective emissivity. We approximate the hemisphere by a sequence of conical surfaces, as depicted in Fig. 2, in front of the main cavity. Every conical segment has its center of curvature coincident with the center of the cavity aperture. The design causes all rays leaving the aperture center that arrive at the concentrator to be retro-reflected.

The concentrator was diamond-turned from aluminum, polished, and gold plated. The reflecting concentrator is mounted on a heat exchanger and its temperature is maintained close to the cavity temperature, but it has no direct thermal contact with the cavity to avoid thermal loading of the latter.

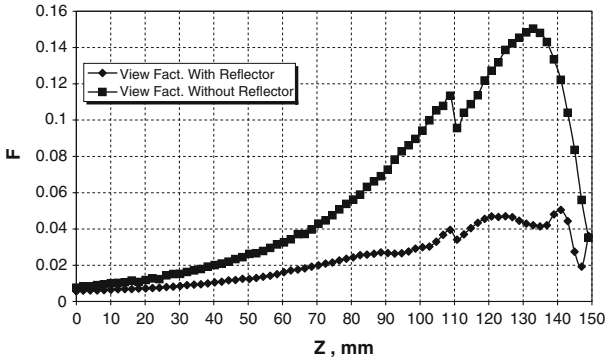


**Fig. 4** Distributions of view factor $F(z)$ along the cavity generatrix computed for cavities with and without a reflecting concentrator

In view of the fact that there are Teflon and copper walls between the gallium and the radiation surface, the temperature drop across the walls needs to be estimated. We assume that there is no radiative heat transfer among the nearly isothermal copper cavity walls, and neglect the thermal radiation emitted from the reflecting concentrator. The flux density $q$ of the cavity-wall heat loss is then equal to

$$q_{\mathrm{r}} = \varepsilon_{\mathrm{wall}}\sigma\left(T_{\mathrm{cavity}}(z)^4 - T_{\mathrm{a}}^4\right)F(z), \tag{1}$$

where $z$ is the axial coordinate, $\varepsilon$ and $T_{\mathrm{cavity}}(z)$ are the hemispherical emissivity and the temperature of the cavity wall at the point with coordinate $z$, respectively, $\sigma$ is the Stefan-Boltzmann constant, $T_{\mathrm{a}}$ is the ambient background temperature, and $F(z)$ is the view factor between the cavity wall at this point and the aperture of the reflecting concentrator, taking into account all multiple reflections inside the cavity and the concentrator. To compute the view factor $F$ for a point on the cavity surface, the Monte Carlo technique was applied [6].

The heat transfer rate from the melting gallium across the walls is given by [9]

$$q_{\mathrm{c}} = k_{\mathrm{eff}}A\frac{(T_{\mathrm{gal}} - T_{\mathrm{cavity}})}{\Delta X}, \tag{2}$$

where $T_{\mathrm{gal}}$ is the temperature of the melting metal, $\Delta X$ is the thickness of the walls, $k_{\mathrm{eff}}$ is the thermal conductivity of the two-layer (copper and Teflon) wall, and $A$ is the inner area of the cavity. Calculation results of the temperature drop $\Delta T$ across the Teflon and cavity walls are presented in Table 1.

The effective emissivity of the cavity with the concentrator was calculated using a Monte Carlo ray-tracing code [6] and determined to be 0.99996. The emissivity is independent of the temperature of the concentrator.

The emissivity of the BB cavity was also evaluated using our infrared total integrated scatter (ITIS) system [10]. The ITIS system consists of infrared laser sources (10.6 μm wavelength in this case), a diffuse gold infrared integrating sphere, pyroelectric and MCT detectors, and a motion control system for manipulating both the

**Table 1** Temperature drop across the Teflon and the cavity walls

| | Mean view factor | Ambient background temperature (K) | $\Delta T$ (K) |
|---|---|---|---|
| Without concentrator | 0.06246 | 77 | 0.153 |
| | | 296 | 0.056 |
| With concentrator | 0.022979 | 77 | 0.013 |
| | | 296 | 0.005 |

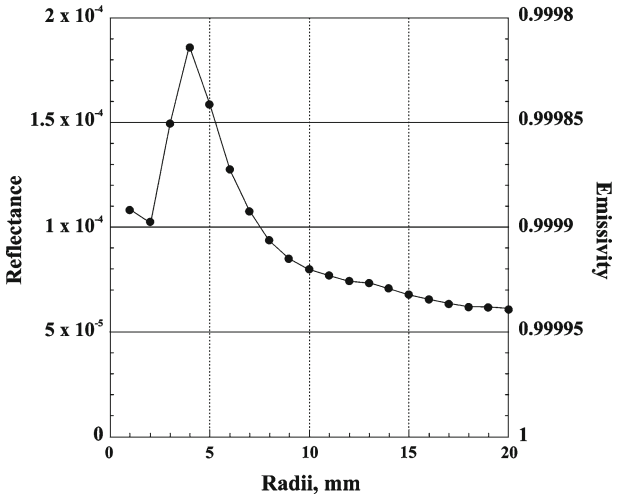


**Fig. 5** Reflectance of the cavity measured using the infrared total integrated scatter system

integrating sphere and the cavity under measurement. The ITIS is used to completely measure the radiation reflected from the cavity under laser illumination from the normal direction. The emissivity $\varepsilon$ is given by $1 - r$, where $r$ is the measured reflectance. The laser beam is nearly collimated with a diameter of about 2 mm. A series of measurements were made, producing a map of the spatial dependence of the emissivity. The data have been integrated to produce the plot showing the variation of cavity emissivity with viewed spot radius, as presented in Fig. 5. The ring spike at a radius of about 6 mm can be explained by an imperfection in the machined cone. Additional details can be found in the companion paper of [10].

## 4 Tunable-Filter Comparator

The radiometric characterization of the BB was performed using the tunable-filter comparator (TFC), which is based on relative radiance measurements [11–13]. Two reference blackbodies of known temperature and emissivity are used for calculation of the system response function. The calculated radiance temperature of the test BB is proportional to the signal from the amplifier and the response function of the system. The TFC contains a small stable internal BB, which is only used as a reference viewed

by a mirror chopper. The technique requires long-term stability of all systems of the TFC.

The output voltages, $V_{\mathrm{ref}1}$, $V_{\mathrm{ref}2}$, from a lock-in amplifier are obtained for two reference blackbodies at known temperatures $T_{\mathrm{ref}1}$, $T_{\mathrm{ref}2}$, and emissivity $\varepsilon_{\mathrm{ref}1}(\lambda)$, $\varepsilon_{\mathrm{ref}2}(\lambda)$. Also, $V_{\mathrm{UUT}}$ is obtained for the tested gallium BB:

$$V_{\mathrm{ref}1} = k\left[\int_{\lambda_1}^{\lambda_2} \varepsilon_{\mathrm{ref}1}(\lambda)L(\lambda, T_{\mathrm{ref}1})S_\lambda d\lambda\right] + V_{\mathrm{bg}}, \tag{3}$$

$$V_{\mathrm{ref}2} = k\left[\int_{\lambda_1}^{\lambda_2} \varepsilon_{\mathrm{ref}2}(\lambda)L(\lambda, T_{\mathrm{ref}2})S_\lambda d\lambda\right] + V_{\mathrm{bg}}, \tag{4}$$

$$V_{\mathrm{UUT}} = k\left[\int_{\lambda_1}^{\lambda_2} L(\lambda, T)S_\lambda d\lambda\right] + V_{\mathrm{bg}}, \tag{5}$$

where $V_{\mathrm{bg}}$ is a combination of all the constant factors, including background and dark current that affect the output voltage. $V_{\mathrm{bg}}$ should be constant during the short measurement time required to obtain the three signals. $S_\lambda$ is the relative spectral responsivity of the system, and $L$ is the spectral radiance according to Planck's radiation law. The coefficient $k$ is determined by the gain and throughput of the system.

From Eqs. 3 and 4, we can calculate $k$ and $V_{\mathrm{bg}}$. Having $k$ and $V_{\mathrm{bg}}$, we obtain the unknown temperature $T_{\mathrm{UUT}}$ by solving Eq. 5 by Newton's method [14]. The optical system of the TFC is shown schematically in Fig. 6. The optical system consists of an aperture stop, a focusing elliptical primary mirror, a reflective chopper, an internal reference BB, a field stop, a continuously variable filter (CVF), a relay mirror, and InSb and HgCdTe (MCT) manually changed detectors. Two water bath-based blackbodies were used as the references with emissivity of 0.99997 and standard uncertainties of (4–8) mK [2]. The TFC instrument enabled us to compare BB radiance temperatures with standard deviations from 5 mK to 15 mK, at temperatures in the range of (10–150) °C, across the (3–5) μm and (8–12) μm atmospheric bands with a relative spectral resolution of (2–3) % ($k = 2$).

## 5 Measurement Results and Discussion

The typical melting cycle of the gallium fixed-point BB and the uniformity of the radiance across the aperture of the BB were measured with the TFC and the results are shown in Figs. 7–9. The temperatures of the two reference water-bath blackbodies during the measurements were 29.875 °C and 23.010 °C. The temperature of the copper heat exchanger was 33.5 °C. In Fig. 7, a melt plateau duration of 7 h was obtained with a variation in stability of less than 10 mK. The uniformity scans shown in Figs. 8 and 9 were performed at a wavelength of 10 μm after the start of melting was identified. The vertical radiance temperature uniformity was found to be ±10 mK and the

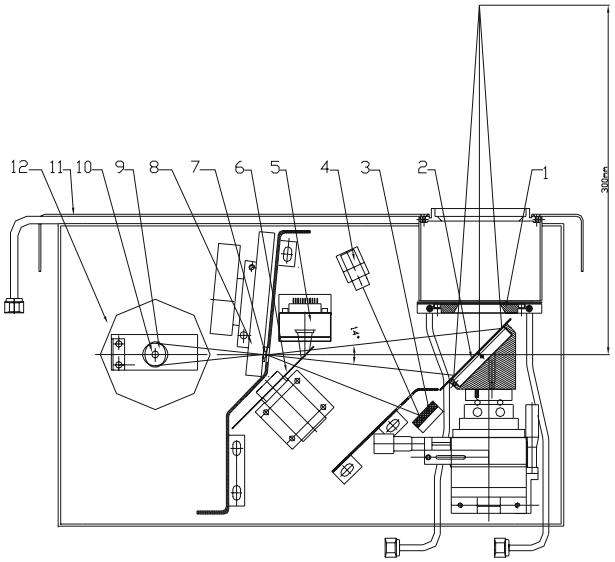


**Fig. 6** Schematic of the TFC. 1: aperture; 2: elliptical mirror; 3: flat mirror; 4: laser; 5: internal blackbody; 6: reflective chopper; 7: field stop; 8: CVF; 9: re-imaging mirror; 10: Lyot stop; 11: front water-cooled wall; 12: down-looking detector with Dewar

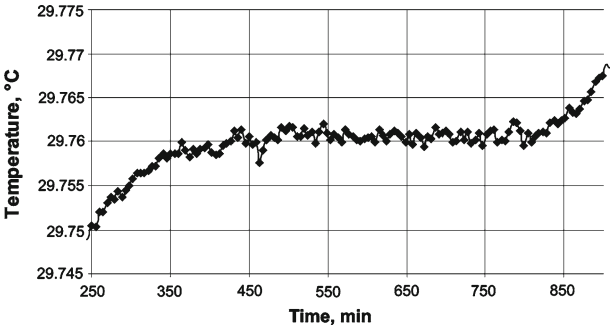


**Fig. 7** Melting plateau

horizontal uniformity was ±5 mK. The spectral radiance temperature was measured by the TFC, and the result is shown in Fig. 10. The radiance temperature at a wavelength of 10 μm was 29.76 °C, and the reproducibility of the temperature was better than 10 mK for different values of the heat exchanger temperatures as shown in Fig. 11. The measured radiance temperature gives an effective emissivity of 0.99992, in good agreement with the predicted value. Calculation of the effective emissivity involves taking into account the room temperature of 23 °C and the temperature drop across the wall. The uncertainty budget for the radiance temperature measurement of the gallium BB is given in Table 2.

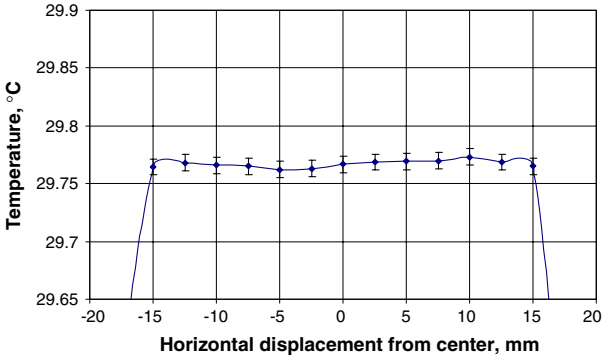


**Fig. 8** Horizontal scan across the aperture during the melt

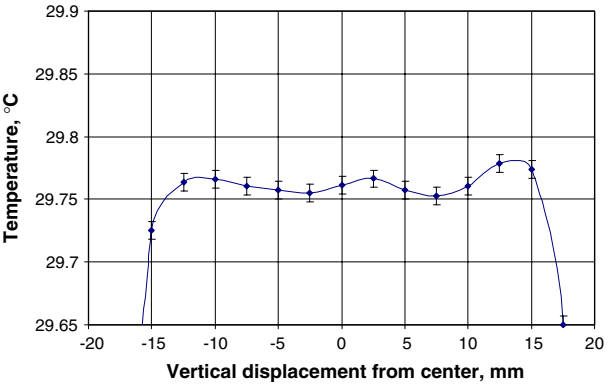


**Fig. 9** Vertical scan across the aperture during the melt

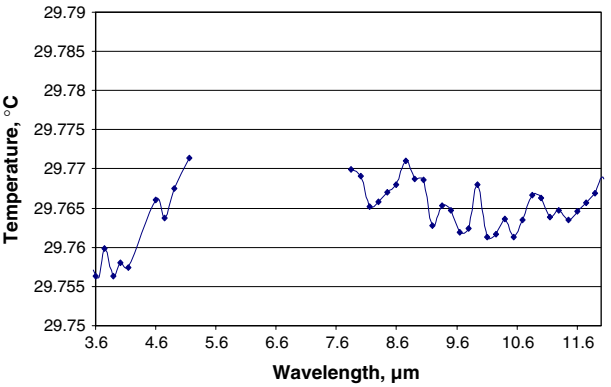


**Fig. 10** Spectral radiance temperature during the melting phase

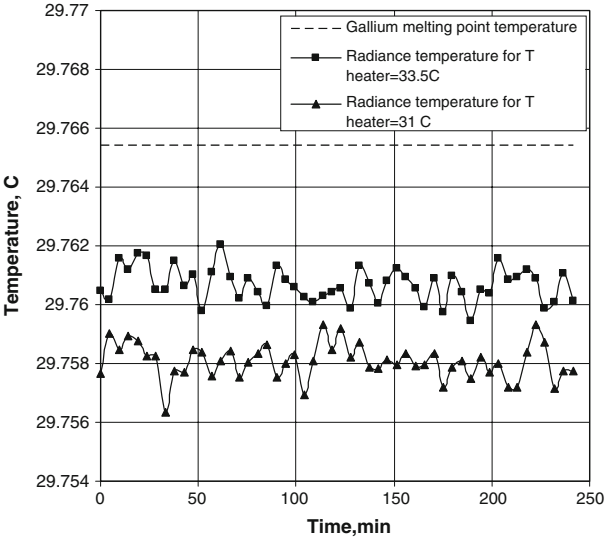


**Fig. 11** At a wavelength of 10 μm, the influence of different heat exchanger temperatures on the radiometric temperature of the melting plateau. Straight line indicates the ITS-90 Ga melting temperature

**Table 2** Uncertainty budget of TFC measurement

| Uncertainty components | $u\,(mK)$ |
|---|---|
| Reference blackbodies | 7 |
| Tunable-filter comparator | 5 |
| Radiance-temperature repeatability | 5 |
| Uniformity, horizontal | 5 |
| Uniformity, vertical | 10 |
| Combined uncertainty ($k = 2$) | 30 |

## 6 Conclusion

A gallium-point BB has been designed, constructed, and tested. It has been demonstrated that a melting duration of 7 h is achieved with a plateau stability and reproducibility on the order of ±0.005 °C. The horizontal non-uniformity of the aperture radiance field is ±0.005 °C and the vertical non-uniformity is ±0.010 °C. The measured radiance temperature is in good agreement with the ITS-90 value of 29.7646 °C, and the only substantial source of uncertainty is the spatial non-uniformity of radiation. The BB has yet to be tested in the environment for which it was mainly intended (cryo-vacuum). Based on our experience with the Ga BB performance, we intend to build similar blackbodies with interchangeable sealed stainless-steel cells containing water and mercury.

**Acknowledgment** The authors like to thank Dr. A.V. Prokhorov for computations specially performed for this work.

## References


1. J. Holland, J. Seidel, R. Klein, G. Ulm, A. Migdal, M. Ware, in *Experimental Methods in the Physical Sciences,* vol. 41, *Optical Radiometry*, ed. by A.C. Parr, R.U. Datla (Elsevier Academic Press, 2005), pp. 234–235
2. J.B. Fowler, J. Res. Natl. Inst. Stand. Technol. **100**, 591 (1995)
3. G. Machin, B. Chu, Meas. Sci. Technol. **9**, 1653 (1998)
4. E. Theocharous, N.P. Fox, V.I. Sapritsky, S.N. Mekhontsev, S.P. Morozova, Metrologia **35**, 549 (1998)
5. M.J. Persky, Rev. Sci. Instrum. **70**, 2193 (1999)
6. V. Sapritsky, A. Prokhorov, Metrologia **43**, 9 (2006)
7. E. Usadi, Metrologia **43**, S1 (2006)
8. T.J. Quinn, J.E. Martin, Metrologia **23**, 111 (1986/1987)
9. A. Gaemi, Appl. Optics **35**, 2211 (1996)
10. L.M. Hanssen, S.N. Mekhontsev, J. Zeng, A.V. Prokhorov, in *Proceedings of TEMPMEKO 2007*. Int. J. Thermophys. **29**, 352 (2008). doi:10.1007/s10765-007-0314-8
11. G. Matis, P. Bryant, J. James, S. McHugh, in *Proceedings of SPIE*, vol. 5407, p. 74 (August 2004)
12. G. Matis, P. Bryant, J. Grigor, J. James, S. McHugh, in *Proceedings of SPIE*, vol. 5784, p. 280 (2005)
13. H. Minato, Y. Ishido, Rev. Sci. Instrum. **74**, 2863 (2003)
14. R.W. Hamming, *Numerical Methods for Scientists and Engineers* (Dover Pubs., New York, 1986), p. 68